Atmospheric Environment 319 (2024) 120279

Contents lists available at ScienceDirect

Atmospheric Environment

journal homepage: www.elsevier.com/locate/atmosenv

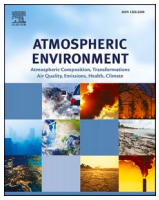

Investigating halogens and MSA in the Southern Hemisphere: A spatial analysis

Delia Segato [a,b,*], Elizabeth R. Thomas [c], Dieter Tetzner [c], Sarah Jackson [i], Dorothea Elisabeth Moser [c,d], Clara Turetta [a,b], Rafael P. Fernandez [e], Alfonso Saiz-Lopez [f], Joel Pedro [g,h], Bradley Markle [j], Andrea Spolaor [a,b]

[a] Department of Environmental Sciences, Informatics and Statistics, Ca' Foscari University of Venice, 155 Via Torino, 30172 Venezia-Mestre, Italy
[b] CNR-Institute of Polar Sciences, 155 Via Torino, 30172 Venezia-Mestre, Italy
[c] Ice Dynamics and Paleoclimate, British Antarctic Survey, Cambridge, CB3 0ET, UK
[d] Department of Earth Sciences, University of Cambridge, Cambridge, CB2 3EQ, UK
[e] Institute for Interdisciplinary Science, National Research Council (ICB-CONICET), FCEN-UNCuyo, Mendoza 5501, Argentina
[f] Department of Atmospheric Chemistry and Climate, Institute of Physical Chemistry Blas Cabrera, CSIC, Madrid, Spain
[g] Australian Antarctic Division, Kingston, TAS, Australia
[h] Australian Antarctic Program Partnership, University of Tasmania, Hobart, TAS, Australia
[i] Research School of Earth Sciences, Australian National University, Canberra ACT 2601, Australia
[j] Institute of Arctic and Alpine Research, Department of Geological Sciences, University of Colorado, Boulder, CO, USA

HIGHLIGHTS

- Sub-Antarctic islands provide unique ice core records.
- Br, Na, MSA and I are highest in the sub-Antarctic region.
- Bromine is depleted in the sub-Antarctic region with respect to coastal Antarctica.
- Iodine reaches is enriched in inner Antarctica following the leapfrog mechanism.

ABSTRACT

Sub-Antarctic islands and Antarctic coastal regions provide valuable sites for investigating environmental processes in the Southern Ocean. The fact that these sites are situated within the sea ice zone underscores their significance in investigating the impact of sea ice on the chemical composition of the boundary layer. In this study we report multi-year average levels of marine aerosols, including bromine, sodium, methanesulphonic acid and iodine, measured in five firn cores collected from sub-Antarctic Islands and coastal Antarctic sites. The records are compared with published Antarctic records to explore the spatial distribution of these species in the Antarctic region and their relationship with sea ice variability. Being mainly sourced from sea-salt aerosols, sodium and bromine exhibit the largest concentrations in the sub-Antarctic region, with progressively reduced deposition from the coast towards the central Antarctic plateau. Due to its gas-phase chemistry, bromine is depleted with respect to sodium in the sub-Antarctic sites. Bromine emitted in the form of sea-salt aerosols undergoes multi-phase recycling in the lower troposphere and, together with gas-phase bromine emitted from sea ice, is likely to be transported away from the source, depositing in enriched concentrations in the plateau compared to the Br/Na sea-water mass ratio. Similarly to bromine and sodium, methanesulphonic acid and iodine are found in higher concentrations in the sub-Antarctic sites, especially where the ocean is sea ice-covered during spring as primary production is stronger than in the ice-free ocean. Sea-salt mediated recycling of gas-phase iodine enhances its atmospheric lifetime, delivering enriched iodine depositions to the Antarctic plateau. Depicting the spatial distribution of these elements is of great importance for understanding the processes delivering these impurities around Antarctica.

1. Introduction

Over the last four decades, the Southern Ocean region has undergone profound changes (Yadav et al., 2022). One key aspect is the establishment of persistent stronger westerly winds around Antarctica (Stammerjohn and Scambos, 2020; Thompson et al., 2011). These atmospheric patterns are thought to be associated with a dramatic sea ice reduction as observed in early 2023 (Purich and Doddridge, 2023).

* Corresponding author. CNR-Institute of Polar Sciences, 155 Via Torino, 30172 Venezia-Mestre, Italy.
E-mail address: delia.segato@unive.it (D. Segato).

https://doi.org/10.1016/j.atmosenv.2023.120279
Received 1 June 2023; Received in revised form 30 November 2023; Accepted 5 December 2023
Available online 9 December 2023

Other than sea ice, atmospheric circulation influences several aspects of the Antarctic environment, including the chemical composition of the atmosphere, the heat transport toward the poles (Sen Gupta and England, 2006), the ocean currents (Herraiz-Borreguero and Naveira Garabato, 2022), as well as the biological activity in Southern Ocean waters (Lovenduski, 2005).

Surface winds are responsible for waves breaking and bubble bursting, releasing significant amounts of sea-salt aerosols containing sodium (Na) and bromine (Br) (de Leeuw et al., 2011). Bromide (Br^-) present in seawater is usually the main source of Br to the atmosphere, but in polar regions atmospheric concentrations can increase following the so-called "bromine explosions", autocatalyzing reaction chains occurring during the sunlit season that lead to the emission of gas-phase bromine species to the boundary layer (Simpson et al., 2007). Such reactions are found to occur at the surface of the first-year sea ice (FYSI), on salty blowing snow over first-year and multi-year sea ice and on sea-salt aerosols produced from frost flowers and salty snow (Huang et al., 2020; Peterson et al., 2019; Pratt et al., 2013). Therefore, a larger FYSI extent results in enhanced reactive Br in the polar boundary layer, which ultimately gets deposited causing the enrichment of bromine in the snowpack compared to the Br/Na sea-water ratio. Bromine enrichment (Br_{enr}) measured in ice cores has been proposed as a tracer of past sea ice variability (Burgay et al., 2023; Spolaor et al., 2016; Vallelonga et al., 2021). This tracer would resolve the issue that Na^+, previously identified as a sea ice proxy (Severi et al., 2017; Wolff et al., 2006), is present in sea-salt aerosols originating from both sea ice and open ocean, and the amount of Na^+ deposited to the Antarctic plateau is strongly influenced by meteorological conditions (E. R. Thomas et al., 2022). However, the complex reactivity of bromine hampers reliable sea ice reconstructions. By examining records from the sub-Antarctic region, we aim to further understand the different transport and deposition pathways of Br species over polar regions and the spatial distribution of Br_{enr}. A better understanding of Br_{enr} distribution in the Southern Ocean region is important for the interpretation of ice core records for reconstructions of sea ice extent beyond satellite observations.

In the Southern Ocean, emissions of methanesulphonic acid (MSA) and iodine (I) are related to both sea ice and biological activity (Curran et al., 2003; Osman et al., 2017; Saiz-Lopez et al., 2015). During the winter season, sea ice expands encircling the Antarctic ice sheet for thousands of kilometers, and almost completely melts away during the summer season. As Antarctic sea ice is almost completely seasonal, it provides microhabitats for the growth of unique sea ice microbial communities, which are an important food resource for secondary and higher-level consumers in the water column (Cowie et al., 2014). These large sea ice variations result in the most productive waters on Earth (Davis and McNider, 1997). MSA is formed in the atmosphere from the oxidation of dimethyl sulfide produced by sea ice algae and the microalgal assemblage in the marginal ice zone (Curran et al., 2003). Therefore, large MSA emissions are expected at the margin of the spring sea ice. Iodine is emitted in both organic and inorganic form from the ocean surface, but seasonally ice-covered areas can emit ~10 times more iodine, as the result of microalgae living underneath and within sea ice releasing iodine species upon oxidative stress induced by light during springtime (Saiz-Lopez et al., 2015). Iodine efflux occurs in sea ice fractures and brine channels, extending all the way to the marine boundary layer. This process is particularly efficient in the Southern Ocean, as most of the sea ice is relatively thin (<50 cm) and frazil, allowing a fast release of iodine through sea ice channels.

Atmospheric and snow concentrations of bromine, sodium, MSA and iodine are the result of a complex interplay of changing patterns of winds, ocean currents, primary productivity and sea ice seasonality in the Southern Ocean (E. R. Thomas et al., 2019). With the aim to investigate the processes of emission, transport and deposition in the Antarctic and sub-Antarctic region, we measured these trace species in five firn cores collected from sub-Antarctic Islands and coastal Antarctic sites (Bouvet, Young, Peter I, Mount Siple islands and Cape Hurley). We compile multi-year averages of available snow and ice records from the Antarctic ice sheet and discuss the processes responsible for distributing these trace species across the Southern Hemisphere.

2. Materials and methods

2.1. Firn core sites

Five firn cores were drilled from sub-Antarctic islands and coastal Antarctic sites as part of the subICE project on board the Antarctic Circumnavigation Expedition cruise in 2017 (Thomas et al., 2021; Walton and Thomas, 2018). These include Bouvet Island, Peter I Island, Mount Siple Island, Young Island and Cape Hurley dome in coastal East Antarctica (Fig. 1).

Bouvet (54° 25′ 19.200″ S, 3° 23' 27.600" E) is a volcanic sub-Antarctic island. The core was drilled on the eastern slope of the island at approximately 350-m altitude to a depth of 14.2 m. Despite being located at a relatively low latitude, surface melting is low, suggesting minimal impact of melt water percolation (E. R. Thomas et al., 2021). The core was dated using annual cycles in concentrations of oxygen isotopes and major ions, resulting in an age scale from 2001 to 2016 for the full core length (King et al., 2019).

Young Island (66° 31′ 44.256″ N, 162° 33′ 35.28″ E, 238 m a.s.l.) is part of the Balleny archipelago and sits in the Antarctic seasonal sea ice zone at the boundary of the polar westerlies and Antarctic coastal easterlies. The Young firn core is the first archive from the Balleny Islands and with its 16.88 m in length covers the period from 1995 to 2016 (Moser et al., 2021). The Young site is strongly affected by melt events, covering 47% of the total depth (E. R. Thomas et al., 2021).

Peter I Island (68° 51′ 50.4″ S, 90° 30′ 54″ W, 730 m a.s.l.) is located in the seasonal sea ice zone of the Bellingshausen and Amundsen Seas. The firn core is 12 m long and covers the period 2002–2016 (E. R. , Thomas et al., 2023).

Mount Siple (Mt Siple, 73° 19′ 14.16″ S, 126° 39′ 47.34″ W, 685 m a.s.l.) is a volcanic island surrounded by the Getz ice shelf. Impurities transported by winds and deposited at Mt Siple can potentially be the result of recent changes in the Amundsen sea low and sea ice conditions in the Bellingshausen and Amundsen Seas. The firn core is 24 m long and presents some visible melt layers (E. R. Thomas et al., 2021; Walton and Thomas, 2018). The period covered by the core is 1998–2016.

Cape Hurley (67° 33′ 34.56″ S, 145° 18′ 45″ E, 320 m a.s.l.) is a low elevation coastal dome adjacent to Mertz Glacier on the George V Coast of East Antarctica. The Mertz glacier tongue, which extends over 100 km, floats on the ocean surface and traps pack ice upstream, forming the third most productive polynya in Antarctica. The Cape Hurley firn core is 20 m long and covers the period 1994–2016 (E. R. Thomas et al., 2021).

2.2. Sample preparation and analyses

The five cores were drilled using a Kovacs Mark II Coring System and transported frozen to the British Antarctic Survey (BAS) in Cambridge (UK) for cutting, sample preparation and analysis. Ice core cutting was performed using a steel band-saw blade in a −25 °C cold lab at BAS. Discrete samples were stored in polypropylene vials that had been precleaned three times by microwaving them filled with Milli-Q water for 5 min. The cores were cut into 5-cm sections. MSA was measured with Ion Chromatography (Thermo Scientific™ Dionex™ Integrion™ HPIC™ system) at BAS using an injection volume of 250 μL in a class-100 cleanroom. For the anion chromatograph, an AG17-C guard column (2 × 50 mm) was used, together with an AS17-C analytical column (2 × 250 mm). Analytical precision, defined as the relative standard deviation of the lowest level standard, is 0.07 ng g^{-1} for MSA.

Additional discrete ice samples were transported to Ca' Foscari university of Venice, Italy, for the analysis of total Br, I and Na and stored frozen. The samples analyzed in Venice had a depth resolution of

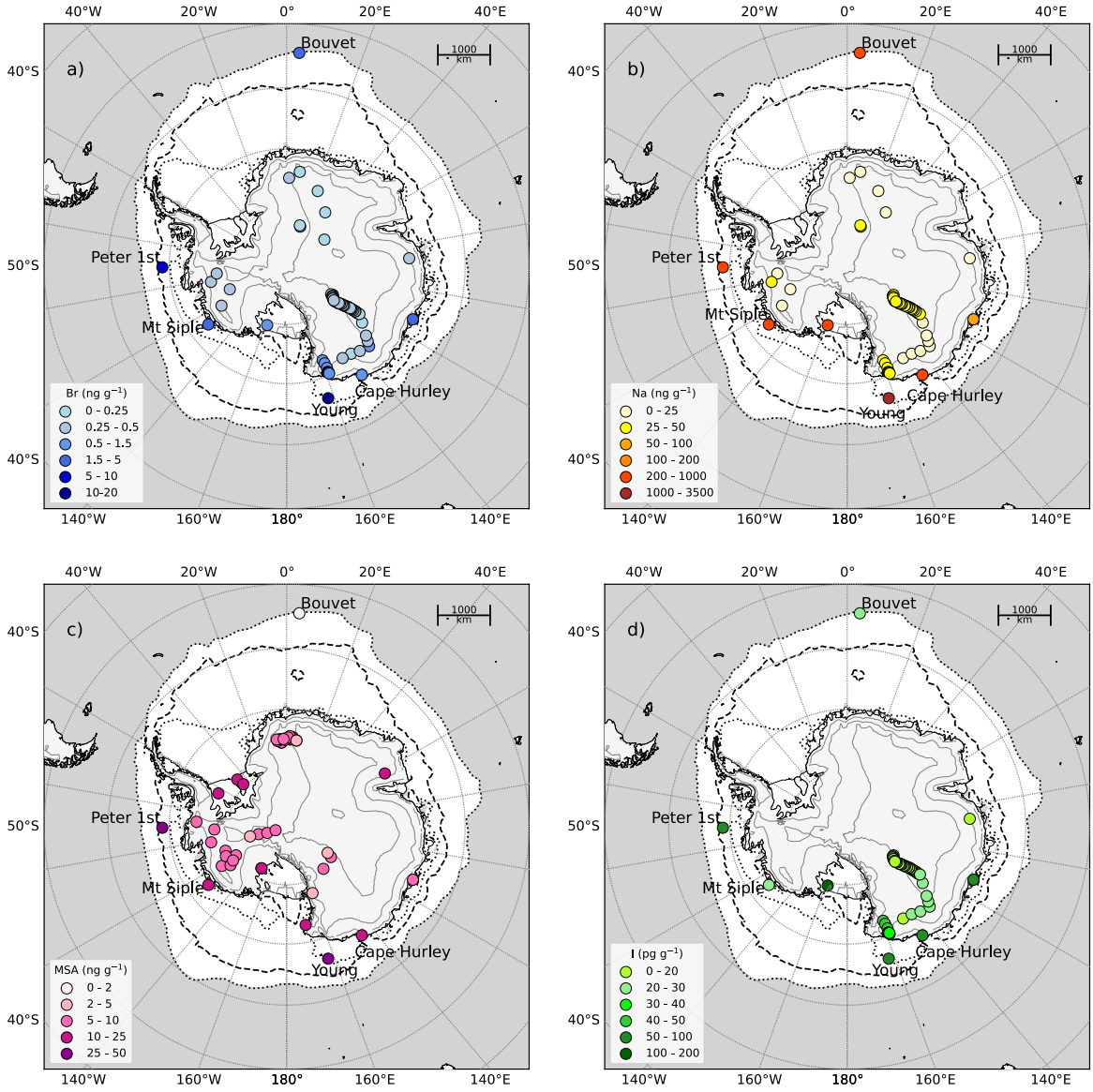

Fig. 1. Spatial variability of Br, Na, MSA and I across Antarctica. a) Br (ng g^{-1}); b) Na (ng g^{-1}); c) MSA (ng g^{-1}); d) I (pg g^{-1}). The black dotted contours represent September (winter) and February (summer) sea ice concentrations 2000–2016. The black dashed line represents December (spring) sea ice concentrations. Sea ice concentrations are retrieved from the National Snow and Ice Data Center (https://nsidc.org/home). Elevation lines are drawn every 1000m.

28 cm for Bouvet, 25 cm for Young, 10 cm for Peter I, Mt Siple and Cape Hurley, with an age coverage of the range ~0.3 years for Bouvet and Young and of ~0.1 years for Peter I, Mt Siple and Cape Hurley. The analysis of Na, Br and I has been conducted at the university of Venice. The sample preparation was done in a class-1000 clean room, under a class-100 laminar flow hood. Total concentrations of Na, Br and I were determined with Inductively Coupled Plasma Mass Spectrometry (ICP-MS). These elements are mainly present in ice core samples as Na^+, Br^- and I^-, while IO_3^- is found to be rarer despite being more stable than I^- (Spolaor et al., 2013). An Inductively Coupled Plasma Single Quadrupole Mass Spectrometer (ICP-SQMS, Thermo Fisher Scientific™ iCAP™ RQ ICP-MS) was used for Bouvet and Young cores in 2019, while Peter I, Mt Siple and Cape Hurley cores were analyzed in 2021 with an Inductively Coupled Plasma Sector Field Mass Spectrometer (ICP-SFMS, Thermo Scientific™ ELEMENT2™). Concentrations were calibrated using external standards and blank-corrected. Standard concentrations ranged from 10 to 5000 ng g^{-1} for Na, 0.1–50 ng g^{-1} for Br, 0.01–5 ng g^{-1} for I. The limit of detection (LOD) of the analyses, defined as three times the standard deviation of the blanks, was 7 ng g^{-1}, 0.44 ng g^{-1} and 0.01 ng g^{-1} for Na, Br and I respectively. A percentage of 100%, 95% and 98% of the samples is higher than the LODs. Reproducibility was evaluated by repeating measurements of ~10% of the samples, showing a percentage difference of 12%, 4% and 24%, for Na, Br and I respectively.

3. Results

Na, Br, MSA and I average levels resulting from our measurements, along with main information on the five firn cores, are displayed in Table 1. The Bouvet MSA record was previously published by King et al. (2019). While several melt layers have been reported in all sub-Antarctic cores (Moser et al., 2021; E. R. Thomas et al., 2021), likely vertically displacing impurities, in this study we consider only the absolute concentrations over multi-year time periods and assume that melt layers do not affect substantially multi-year average concentrations (Moore et al., 2005). To evaluate the spatial variability of the deposition of these species in snow, a compilation of multi-year averages is made including results from this study and ice core records from the Antarctic ice sheet

Table 1
Average and 95% confidence level of Na, Br, MSA and I in the Bouvet, Young, Peter I and Mt Siple and Cape Hurley firn cores. The table also includes the main details on the drilling locations and firn core properties.

Firn core	Bouvet	Young	Peter I	Mt Siple	Cape Hurley
Age cover (CE)	2001–2016	1995–2016	2002–2016	1998–2016	1994–2016
Latitude	54° 25′ 19.20″ S	66 31′ 44.3″ S	68° 51′ 50.4″ S	73° 19′ 14.16″ S	67° 33′ 34.56″ S
Longitude	3° 23′ 27.600″ E	162 33′ 21.5″ E	90° 30′ 54″ W	126° 39′ 47.34″ W	145° 18′ 45″ E
Elevation (m a.s.l.)	350	238	730	685	320
Ice core length (m)	14.05	16.92	12.25	24.13	20.22
Snow accumulation (kg m^{-2} y^{-1})	715	506	484	600	590
Na (ng g^{-1})	543 ± 120	3290 ± 400	896 ± 110	453 ± 42	342 ± 36
Br (ng g^{-1})	2.2 ± 0.4	15 ± 2	5.3 ± 0.7	2.4 ± 0.2	0.9 ± 0.1
MSA (ng g^{-1})	1.9 ± 0.4	40 ± 4	34 ± 7	22 ± 2	19 ± 2
I (pg g^{-1})	32 ± 5	82 ± 18	67 ± 15	24 ± 4	50 ± 11

(Fig. 1). When available, the averages are calculated considering the most recent 20 years covered by each core. Published Antarctic ice core records were retrieved from different locations of the plateau: Talos Dome to GV7 traverse (Maffezzoli et al., 2017), Law Dome (Vallelonga et al., 2021), Talos Dome to Dome C traverse (Vallelonga et al., 2021), Dome C (Burgay et al., 2023), EAIIST (East Antarctic International Ice

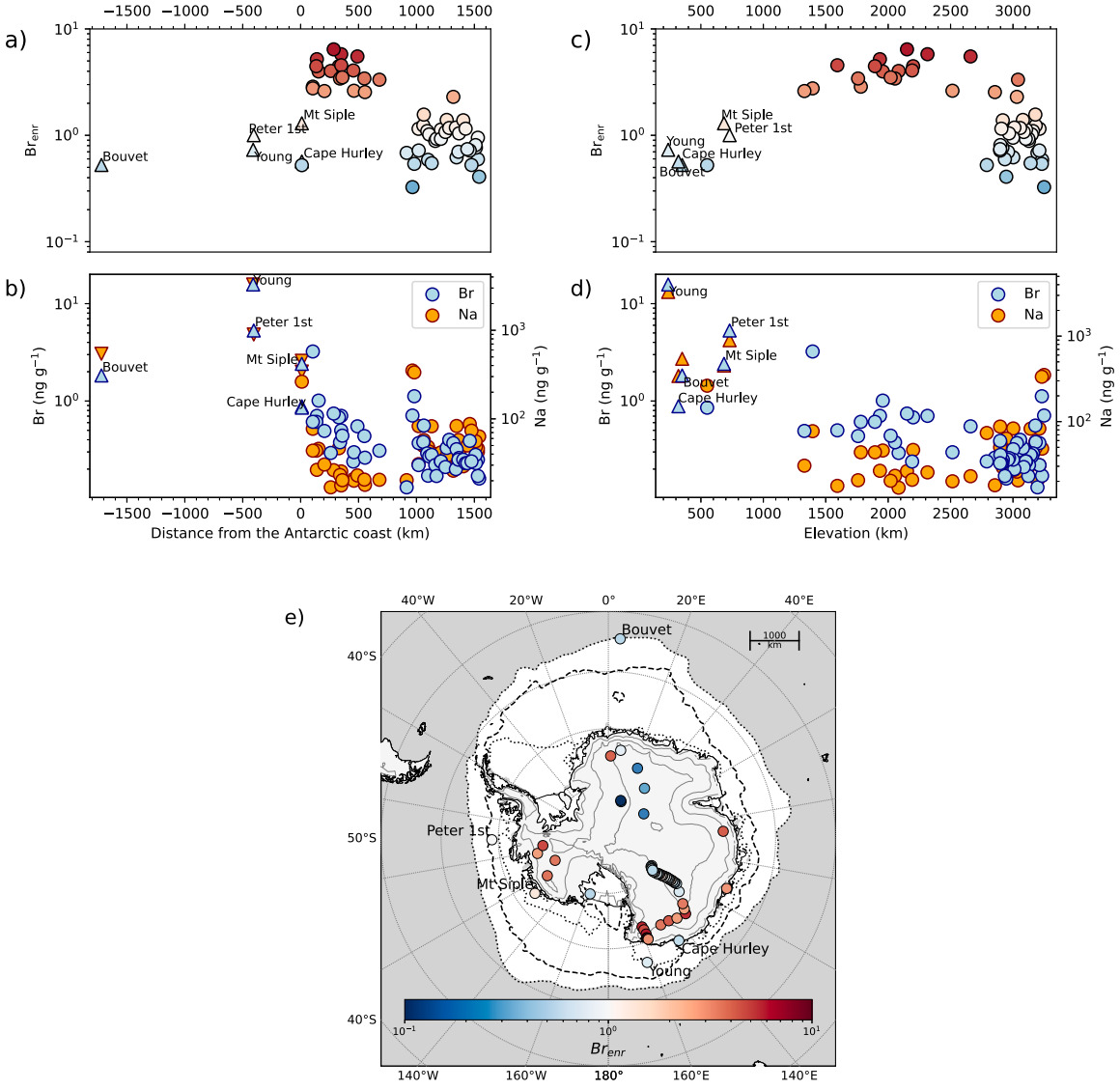

Fig. 2. Snowpack concentrations of Br_{enr}, Br and Na with respect to the distance from the Antarctic coastline. Panel a) Br_{enr} vs distance from the Antarctic coastline (km). Negative distance values indicate sites located in the Southern Ocean, positive values indicate sites located in the Antarctic ice sheet. Only sites for which both Na and Br have been measured are shown here. Panel b) Br (ng g^{-1}) and Na (ng g^{-1}) vs distance from the Antarctic coastline (km). Panel c) Br_{enr} vs elevation (m a.s.l.); Panel d) Br (pg g^{-1}) and Na vs elevation (m a.s.l.); Panel e) Representation of spatial Br_{enr} variability in the Antarctic region. The black dotted contours represent September (winter) and February (summer) sea ice concentrations 2000–2016. Sea ice concentrations are retrieved from the National Snow and Ice Data Center. Elevation contour lines are drawn every 1000m.

Sheet Traverse) traverse (Celli et al., 2023), individual sites in West Antarctica (McConnell et al., 2014), Dronning Maud Land (Weller et al., 2004), and Roosevelt Island (RICE ice core) (Vallelonga et al., 2021). Additionally, Na and MSA ions measured in shallow cores retrieved during the US International Trans-Antarctic Scientific Expedition (US ITASE) are available at https://www.icecoredata.org/cci/Antarctica.html (Sneed et al., 2011). The database also contains data from additional cores such as Dominion range (Mayewski et al., 1995), Taylor Dome (Mayewski et al., 1996), Siple Dome A (Mayewski et al., 2013), and Detroit Plateau (Potocki et al., 2016). Finally, a compilation of Na and MSA ions has been published in Osman et al. (2017).

All tracers present their largest values at Young, followed by Peter I, highlighting that the largest concentrations are over regions that every year are completely surrounded by FYSI (Table 1). On the other hand, Mt Siple and Cape Hurley are located on the coast of the Antarctic continent and have a larger influence of MYSI, while Bouvet lies on the edge of the sea-ice coverage during the winter. In comparison with records from the Antarctic ice sheet, bromine and sodium have a larger concentration in sub-Antarctic and coastal sites (Fig. 1a,b) in comparison to the continental ice sheet. This is in agreement with observations by Bertler et al. (2005), Simpson et al. (2005), Maffezzoli et al. (2017) and Vallelonga et al. (2021). Bromine concentration at sub-Antarctic to coastal locations ranges from 1.5 to 16 ng g^{-1} while sodium concentration ranges from 50 to 3300 ng g^{-1}. Bromine and sodium generally show lower concentrations on the inner plateau, with Br ranging from 0.1 to 1.5 ng g^{-1} and Na ranging from 17 to 50 ng g^{-1}. Bromine enrichment ($Br_{enr} = [Br]_{snow}/([Na]_{snow} \bullet [Br/Na]_{seawater}$), instead, shows a different spatial pattern with levels ≤ 1 at the sub-Antarctic islands further from the coast (Bouvet, Young and Peter I) and >1 at coastal to continental Antarctic locations (Fig. 2). Br becomes again depleted in the sites located furthest from the coast (>600 km) with $Br_{enr} \leq 1$, similarly to the sub-Antarctic sites. These sites are also the one with the highest elevation ~3000 m a.s.l.

MSA concentration has a spatial pattern similar to that of Na and Br,

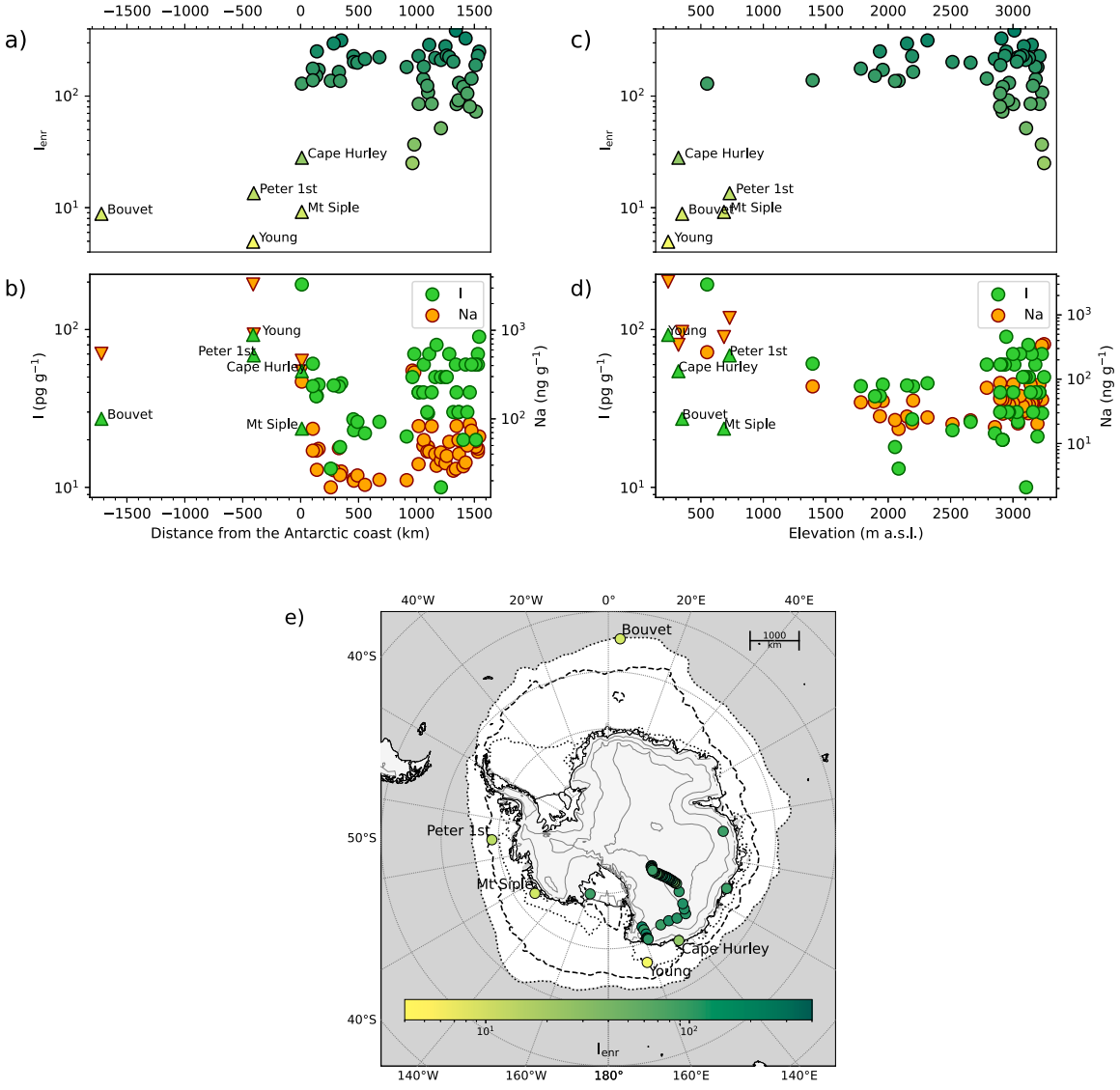

Fig. 3. Snowpack concentrations of I_{enr}, I and Na with respect to the distance from the Antarctic coastline and elevation. Panel a) I_{enr} vs distance from the Antarctic coastline (km). Negative distance values indicate sites located in the Southern Ocean, positive values indicate sites located in the Antarctic ice sheet. Only sites for which both Na and I have been measured are selected. Panel b) Same but for I (pg g^{-1}) and Na (ng g^{-1}); Panel c) I_{enr} vs elevation (m a.s.l.); Panel d) I (pg g^{-1}) and Na vs elevation (m a.s.l.); Panel e) Representation of I_{enr} spatial variability in the Antarctic region. The black dotted contours represent September (winter) and February (summer) sea ice concentrations. The red dashed line represents December (spring) sea ice concentrations. Sea ice concentrations are retrieved from the National Snow and Ice Data Center. Elevation lines are drawn every 1000m.

with larger concentrations close to marine sources and progressively lower concentrations going inland toward the inner ice sheet (Fig. 1c). In fact, the largest concentrations are found at sub-Antarctic sites like Peter I, Mt Siple and Young cores, with 34, 22 and 40 ng g^{-1}, respectively. Lower concentrations are found at coastal sites (i.e. 10 – 25 ng g^{-1} in the Ronne ice shelf), while the lowest concentrations are found inland, with a range of ~2–10 ng g^{-1}. The iodine concentration range is between 20 and 200 pg g^{-1} in the sub-Antarctic to coastal region (Fig. 1d). Consistently, lower concentrations are instead found in the inner plateau, with a range between 13 and 40 pg g^{-1}. Interestingly, considering iodine enrichment with respect to sea-water mass ratio (calculated as $I_{enr} = [I]/([Na] \bullet 5.6 \bullet 10^{-6})$, higher levels are evident in the inner plateau (Fig. 3). There, iodine is enriched more than 300 times, further evidencing a different emission and transport pathway with respect to sea-salt Na.

It must be noted, however, that any spatial pattern of these concentrations is affected by local features such as annual snow accumulation, distance from the coast and elevation. There are no clear associations between snowpack chemistry of these tracers and accumulation rate, despite several studies were conducted on the topic (Abram et al., 2013). In our case, concentrations and fluxes are positively correlated, meaning that the change in accumulation is not the main driver of the spatial distribution of these species. Also, from the emission source to the deposition site, atmospheric circulation, topography and precipitation patterns modify the trajectory of air masses and influence the distance at which trace species are deposited. The interaction between these processes makes it challenging to pinpoint the singular influence of any one factor on the spatial distribution of trace species.

4. Discussions

4.1. Bromine and sodium in sub-Antarctic firn cores

In the sub-Antarctic region (e.g., Bouvet), Br and Na are mostly emitted to the polar boundary layer in the form of sea-salt aerosols lifted from the unfrozen Southern Ocean (M. A. Thomas et al., 2022). Both Br and Na are deposited in greater concentrations at sub-Antarctic and coastal sites as they are close to the sources of emission (Fig. 1a,b), while the concentrations are gradually lower when moving inland. Similar results were previously found by Bertler et al. (2005), where Na^+ shows larger concentrations at coastal sites. The atmospheric residence time of sea-salt aerosols is estimated to be of a few days (Schüpbach et al., 2018), implying deposition of most aerosol-phase Br and Na relatively close to the source of emission and lower levels transported for long distances. The production of sea-salt aerosols is strongly influenced by surface wind speed (Liu et al., 2021). Therefore, how much of these elements is deposited and preserved in sub-Antarctic glaciers may be proportional to past wind strength variability. However, bromine in the atmosphere does not only stem from sea-salt aerosols, but it is also emitted in organic form from the open ocean and as reactive gas from the sea ice during bromine explosion events. Instead, Na only occurs in aerosol phase and its low reactivity makes it better suited for reconstructions of past wind variability.

Br_{enr} presents a different spatial pattern with respect to that of Br and Na (Fig. 2e). In the sub-Antarctic region, particularly in ocean areas covered by sea ice during spring, Br_{enr} levels are on average smaller than 1, indicating a zone of depletion of bromine species compared to sea-water ratio in the snowpack. Here, bromine is activated over sea ice surfaces or on salty blowing snow above sea ice, emitting reactive gas-phase inorganic Br species (Br_y) to the boundary layer (Marelle et al., 2021). Br_y can then be taken up by particles and liberate more halogens from the condensed phase (Krnavek et al., 2012; Saiz-Lopez and von Glasow, 2012). The multiphase chemistry of bromine is such that a bromine atom may undergo several aerosol-gas phase exchanges during its transport. Given that the recycling of bromine is efficient primarily over FYSI, these cycles of reactions can sustain gas-phase bromine in the boundary layer over longer periods than sodium, which exists only in aerosol phase and is not involved in chemical reaction chains. Therefore, bromine species emitted from sea ice are likely transported by atmospheric circulation and deposited in enriched concentrations on the interior of the ice-sheet (Vallelonga et al., 2021). This behavior is supported by a 1-D chemistry model simulation by Spolaor et al. (2016), which predicted an increase of bromine deposition on the snowpack after 24–48 h of bromine recycling over sea ice. During this time, sea ice-sourced bromine can be transported south and reach inner Antarctica where it deposits in enriched amounts with respect to the sea-water ratio due to its longer atmospheric lifetime, as previously reported at Alert, Canada (Toom-Sauntry and Barrie, 2002). Vallelonga et al. (2021) stated, based on snow and ice measurements, that Br_{enr} progressively increases from the coast proceeding inland, where it reaches peak values at a distance of 300–600 km from the coast. In central Antarctica, at distances >600 km from the coast, Br_{enr} becomes again depleted, possibly because gas-phase Br concentrations in the boundary layer are too low to sustain an efficient Br reactivity and only aerosols strongly depleted in Br reach the central plateau (Vallelonga et al., 2021). Similarly, considering the relation between Br_{enr} variability and the elevation at which observations are taken, we find that the highest Br_{enr} levels are found at sites in coastal Antarctica at an elevation between ~1500 and 2500 m above sea level (Fig. 2c). However, while it is difficult to distinguish between the effects of Br_{enr} levels being influenced by the distance from the coast versus elevation, it appears that this ratio changes in a steeper way with changing distance from the coast, suggesting this process to have a stronger influence. In this context, the depletion of bromine we find in the sub-Antarctic cores suggests that a great fraction of bromine is suspended in gas-phase in the boundary layer over the Southern Ocean, matching satellite measurements (Schönhardt et al., 2012). Further inland, Br reactivity is less efficient and bromine-poor sea-salt aerosols get deposited over the Antarctic plateau.

Thus, for the purpose of investigating past trends or changes in wind patterns around Antarctica using ice core records, Na deposition in sub-Antarctic sites may be used for investigating past changes in wind patterns and distance to the sea ice margin. However, the hydrological cycle constitutes the primary driver of sea salt aerosols removal from the atmosphere, and its changes must be carefully considered when interpreting records of sea-salt aerosols (Markle et al., 2018). For investigating past sea ice variability, ice cores retrieved in the coastal Antarctic plateau should be considered, as the enrichment in Br with respect to sea-water ratio is likely to be proportional to sea ice related bromine chemistry, i.e. the larger the FYSI extension, the more efficient bromine recycling and the larger increase in Br_{enr} at the coast. Even though bromine chemistry is influenced by polar processes including light availability and boundary layer dynamics influencing emission, recycling and deposition of bromine (Marelle et al., 2021), Br_{enr} in coastal sites may give an indication of past sea ice variability when considering periods of decadal to centennial time scales.

4.2. Iodine and MSA in sub-Antarctic firn cores

In the Southern Ocean region, MSA and iodine concentration in the atmosphere is related to sea ice and biogenic activity (Curran et al., 2003; Saiz-Lopez et al., 2015; Welch et al., 1993). The highest MSA concentrations are found in the sub-Antarctic area, especially in the Young and Peter I cores (40 and 34 ng g^{-1}, respectively). High concentrations are also deposited at coastal sites and ice shelves, while they decrease proceeding inland (Fig. 1c). MSA concentration in Bouvet Island is comparatively low (1.9 ng g^{-1}), likely because the site is located at the edge of the winter sea ice, while sea ice algae are found to be most productive after sea ice decay, in the spring/summer marginal sea ice zone (Fig. 1c) close to the Antarctic coast (Curran et al., 2003). Higher concentrations of MSA along the spring sea ice are in line with previous

observations (Bertler et al., 2005; Osman et al., 2017) and modeling (Hezel et al., 2011), which report decreasing MSA with increasing distance from the marine source. This spatial distribution is also caused by post-depositional loss processes of MSA from low accumulation continental sites (Abram et al., 2013). In this line of reasoning, MSA deposited in sub-Antarctic sites lying in the spring-to-summer marginal sea ice zone is representative of the in-situ biological productivity and measurements conducted in ice retrieved from sub-Antarctic regions is comparatively less influenced by loss along transport toward the Antarctic ice sheet.

In a similar way, iodine concentrations are higher in coastal and sub-Antarctic sites. Here, high levels of iodine released from sea ice areas into the atmosphere result in high concentrations of iodine species deposited directly at these sites. Mt Siple and Bouvet iodine concentrations (24 and 32 pg g^{-1}, respectively) are however lower than Young, Peter I and Cape Hurley (82, 67 and 50 pg g^{-1}, respectively). The hypothesis for lower concentrations at Bouvet is that this island is located outside the spring sea ice zone, where westerly winds move around impurities reflecting the ice-free ocean conditions, which are poorer in iodine content. In addition, the oceanic HOI/I_2 source due to iodide oxidation occurring at the seawater surface (Carpenter et al., 2013; Prados-Roman et al., 2015) is also reduced due to the low ozone abundance prevailing at the high latitudes of the Southern Hemisphere. Lower levels deposited at Mt Siple may be related to the neighboring ocean being mostly covered by MYSI and in an area with comparatively lower primary productivity, as well as the site being located at a high elevation (685 m a.s.l.). Low iodine concentrations are found in the inner plateau, ranging between 18 and 45 pg g^{-1}, which can easily be explained by the increasing distance from the source areas of emission and lower precipitation (Turner et al., 2019). However, it should be highlighted that the reduction in iodine concentrations from the coast to the interior is at most a factor of 10 (Fig. 3b) while for the case of bromine the decrease in Br concentrations from the coast to the interior can be larger than a factor of 100 (Fig. 2b). This highlights that iodine has a much more reactive recycling efficiency on the snowpack because of low snow accumulation and of post-depositional processes induced by UV radiation which take place for iodine species, but are not observed for bromine (Burgay et al., 2023; Li et al., 2022; Spolaor et al., 2021).

To understand the behavior of iodine in the atmosphere, we consider iodine enrichment with respect to sea-salt sodium, as the latter does not participate in halogen reactions. Higher I/Na ratios are found in inner Antarctica (Fig. 3a), which coincides with the highest elevations (Fig. 3c). These high levels are likely explained, similarly to bromine species, by the gas-phase iodine recycling on sea salt-aerosols, enhancing its atmospheric lifetime (Saiz-Lopez et al., 2008). Additionally, high levels may be explained considering the fate of iodine once deposited in snow. Iodine in the snowpack is mostly in the ionic forms of iodide (I^-) and iodate (IO_3^-), which are strongly photoactive in snow matrices (Spolaor et al., 2021). UV radiation photoactivates iodine species producing I_2 and I_3^-, which are released to the atmosphere (Kim et al., 2016). Iodine species are then deposited as iodine reservoirs and undergo heterogeneous recycling in ice (photo-oxidation of iodide and photoreduction of iodate) and re-emission of active gaseous iodine to the atmosphere, which initiates the process again (Fernandez et al., 2019). This mechanism is called “leapfrog” and allows the transport of iodine from the coast to the interior of Antarctica, thereby reproducing satellite observations of enhanced IO over inner areas such as the Ronne and Ross ice-shelves (Schönhardt et al., 2012). These cycles of deposition, recycling and re-emission of iodine could explain the enrichment of iodine in inner Antarctica with respect to sea-salt Na measured in ice cores. Observations of iodine in sub-Antarctic sites, therefore, support the hypothesis of long-range transport of iodine, reaching far inside the Antarctic plateau.

5. Conclusions

Here, we have presented multi-year average levels of Br, Na, MSA and I measured in five sub-Antarctic and Antarctic coastal sites. The chemistry of these elements is linked to oceanic processes in the Southern Ocean region and atmospheric patterns, responsible for uplifting and transporting trace species. The five cores were retrieved from the Bouvet, Young, Peter I and Mt Siple islands, and a coastal site near Mertz glacier. By comparing our measurements with published Antarctic records, we evaluate the spatial variability of these species. We find higher levels of Br, Na, MSA and I at these sites with respect to the Antarctic ice sheet. This study helps to expand our knowledge of the emission, transport and deposition processes of these species in a previously unexplored region.

Br and Na show the highest levels in the sub-Antarctic region and progressively lower values proceeding inland, in line with previous studies. Na and Br deposited in sub-Antarctic sites are likely to be influenced by winds lifting sea-salt aerosols from the ocean and sea ice surface and may vary concomitantly with changes in atmospheric circulation patterns. Br_{enr}, instead, appears to be depleted or close to seawater ratio in sub-Antarctic and coastal sites. This can be explained through the reactivity of gas-phase Br species, which are involved in heterogeneous recycling and remain suspended in the atmosphere, travelling longer distances than sea-salt bromide. In coastal to inner Antarctic sites, Br is enriched in the snowpack, reflecting effective transport of Br species originated from sea ice processes that are deposited over the snowpack. Therefore, when considering Br_{enr} for past sea ice reconstructions, these sites may be better suited than sub-Antarctic islands. More inland, Br_{enr} is again depleted, probably because Br heterogenous chemistry is less efficient.

We find relatively high levels of MSA deposition in the sub-Antarctic and coastal region, probably as a result of MSA production in the spring sea ice area during spring phytoplankton bloom. Progressively lower levels are deposited proceeding toward the Antarctic interior due to loss along transport and to post-depositional processes within the snow, in line with previous studies. Compared to other sub-Antarctic sites, concentration levels are lower at Bouvet Island situated near the margin of Antarctic winter sea ice, because the site is outside the primary production zone near spring sea ice break-up. Future Antarctic sea ice decline in the coming years, with 2022 hitting the lowest minimum record, may have consequences for biological production in the Southern Ocean, as shown by higher MSA and iodine within the spring sea ice zone.

Iodine depositions show a similar pattern compared to MSA, however, few observations are available and are not homogeneously distributed in the sub-Antarctic and Antarctic region. Considering the iodine enrichment with respect to sea-salt aerosols, we find levels two orders of magnitude higher in inner Antarctica with respect to the sub-Antarctic region. Iodine recycling on sea-salt aerosols, together with the photoactivity of iodine on snow and ice allows its transport for longer distances than sea-salt aerosols. Further, the iodine recycling efficiency and its photo-activation in the snowpack allow iodine species to be transported inland more efficiently than bromine. An evaluation of the spatial pattern of iodine deposition requires further in-situ observations, as well as satellite observations and modelling of iodine transport.

In their ability to capture atmospheric and oceanic processes in the Southern Ocean, such as changes in biological productivity and sea ice extent, sub-Antarctic glaciers and ice caps hold precious information about changing climate in the Southern Hemisphere. Considering the record minimum in sea ice observations in the Southern Ocean in 2023, delving into these processes becomes particularly important for anticipating future developments in the Antarctic region. To gain a deeper understanding, future research efforts should focus on analyzing subseasonal trends of trace species preserved in the ice layers of these glaciers. Additionally, conducting drilling campaigns to retrieve centennial-long ice cores can provide valuable insights into past climate

variability in the Southern Ocean region. This comprehensive approach will contribute to our knowledge of the complex and dynamic climate system in the Southern Hemisphere.

CRediT authorship contribution statement

Delia Segato: Conceptualization, Investigation, Writing – original draft. **Elizabeth R. Thomas:** Conceptualization, Funding acquisition, Resources, Writing – review & editing. **Dieter Tetzner:** Writing – review & editing. **Sarah Jackson:** Investigation, Writing – review & editing. **Dorothea Elisabeth Moser:** Writing – review & editing. **Clara Turetta:** Investigation. **Rafael P. Fernandez:** Writing – review & editing. **Alfonso Saiz-Lopez:** Writing – review & editing. **Joel Pedro:** Writing – review & editing. **Bradley Markle:** Writing – review & editing. **Andrea Spolaor:** Conceptualization, Funding acquisition, Supervision, Writing – review & editing.

Declaration of competing interest

The authors declare that they have no known competing financial interests or personal relationships that could have appeared to influence the work reported in this paper.

Data availability

Data will be made available on request.

Acknowledgements

Funding for the subICE campaign was provided by École Polytechnique Fédérale de Lausanne, the Swiss Polar Institute, and Ferring Pharmaceuticals Inc. E.R.T. received core funding from the Natural Environment Research Council to the British Antarctic Survey's Ice Dynamics and Paleoclimate Programme. The authors are grateful to the Norwegian Polar Institute for granting permission to visit Peter I and Bouvet Island. The authors would also like to acknowledge the co-ordinators and participants of the Antarctic Circumnavigation Expedition for facilitating collection of the subICE cores, especially David Walton, Christian de Marliave, Julia Schmale, Guisella Gacitúa, Amy King, Roger Stilwell, and Frederick Paulsen. Funding was also provided by the Programma Nazionale per la Ricerca in Antartide (PNRA; project no. PNRA16_00295), and by the bilateral international exchange award Royal Society (UK)-CNR, titled "Antarctic sea-ice history: developing robust ice core proxies" (grant no. IEC/R2/202110), awarded to Rachael H. Rhodes and Andrea Spolaor. This work contributes to the Antarctic Science Collaboration Initiative program (project ID ASCI000002).

References

Abram, N.J., Wolff, E.W., Curran, M.A.J., 2013. A review of sea ice proxy information from polar ice cores. Quat. Sci. Rev. 79, 168–183. https://doi.org/10.1016/j.quascirev.2013.01.011.

Bertler, N., Mayewski, P.A., Aristarain, A., Barrett, P., Becagli, S., Bernardo, R., Bo, S., Xiao, C., Curran, M., Qin, D., Dixon, D.A., Ferron, F., Fischer, H., Frey, M., Frezzotti, M., Fundel, F., Genthon, C., Gragnani, R., Hamilton, G.S., et al., 2005. Snow chemistry across Antarctica. Ann. Glaciol. 41, 167–179. https://doi.org/10.3189/172756405781813320.

Burgay, F., Fernández, R.P., Segato, D., Turetta, C., Blaszczak-Boxe, C.S., Rhodes, R.H., Scarchilli, C., Ciardini, V., Barbante, C., Saiz-Lopez, A., Spolaor, A., 2023. 200-year ice core bromine reconstruction at Dome C (Antarctica): observational and modelling results. Cryosphere 17 (1), 391–405. https://doi.org/10.5194/tc-17-391-2023.

Carpenter, L.J., MacDonald, S.M., Shaw, M.D., Kumar, R., Saunders, R.W., Parthipan, R., Wilson, J., Plane, J.M.C., 2013. Atmospheric iodine levels influenced by sea surface emissions of inorganic iodine. Nat. Geosci. 6 (2), 108–111. https://doi.org/10.1038/ngeo1687.

Celli, G., Cairns, W.R.L., Scarchilli, C., Cuevas, C.A., Saiz-Lopez, A., Savarino, J., Stenni, B., Frezzotti, M., Becagli, S., Delmonte, B., Angot, H., Fernandez, R.P., Spolaor, A., 2023. Bromine, iodine and sodium along the EAIIST traverse: Bulk and surface snow latitudinal variability. Environ. Res. 239, 117344 https://doi.org/10.1016/j.envres.2023.117344.

Cowie, R., Williams, G., Maas, E., Voyles, K., Ryan, K., 2014. Antarctic sea-ice microbial communities show distinct patterns of zonation in response to algal-derived substrates. Aquat. Microb. Ecol. 73 (2), 123–134. https://doi.org/10.3354/ame01710.

Curran, M.A.J., Ommen, T. D. Van, Morgan, V.I., 2003. Ice core evidence for Antarctic sea ice decline since the 1950s, 302 (November), 1203–1207.

Davis, A.M.J., McNider, R.T., 1997. The development of Antarctic Katabatic winds and implications for the coastal ocean. J. Atmos. Sci. 54 (9), 1248–1261. https://doi.org/10.1175/1520-0469(1997)054<1248:TDOAKW>2.0.CO;2.

de Leeuw, G., Andreas, E.L., Anguelova, M.D., Fairall, C.W., Lewis, E.R., O'Dowd, C., Schulz, M., Schwartz, S.E., 2011. Production flux of sea spray aerosol. Rev. Geophys. 49 (2), 1–39. https://doi.org/10.1029/2010RG000349.

Fernandez, R.P., Carmona-Balea, A., Cuevas, C.A., Barrera, J.A., Kinnison, D.E., Lamarque, J.F., Blaszczak-Boxe, C., Kim, K., Choi, W., Hay, T., Blechschmidt, A.M., Schönhardt, A., Burrows, J.P., Saiz-Lopez, A., 2019. Modeling the sources and chemistry of polar tropospheric halogens (Cl, Br, and I) using the CAM-Chem global chemistry-climate model. J. Adv. Model. Earth Syst. 11 (7), 2259–2289. https://doi.org/10.1029/2019MS001655.

Herraiz-Borreguero, L., Naveira Garabato, A.C., 2022. Poleward shift of Circumpolar deep water threatens the East Antarctic ice sheet. Nat. Clim. Change 12 (8), 728–734. https://doi.org/10.1038/s41558-022-01424-3.

Hezel, P.J., Alexander, B., Bitz, C.M., Steig, E.J., Holmes, C.D., Yang, X., Sciare, J., 2011. Modeled methanesulfonic acid (MSA) deposition in Antarctica and its relationship to sea ice. Journal of Geophysical Research Atmospheres 116 (23). https://doi.org/10.1029/2011JD016383.

Huang, J., Jaeglé, L., Chen, Q., Alexander, B., Sherwen, T., Evans, M.J., Theys, N., Choi, S., 2020. Evaluating the impact of blowing-snow sea salt aerosol on springtime BrO and O3 in the Arctic. Atmos. Chem. Phys. 20 (12), 7335–7358. https://doi.org/10.5194/acp-20-7335-2020.

Kim, K., Yabushita, A., Okumura, M., Saiz-Lopez, A., Cuevas, C.A., Blaszczak-Boxe, C.S., Min, D.W., Yoon, H.-I., Choi, W., 2016. Production of molecular iodine and Tri-iodide in the frozen solution of iodide: implication for polar atmosphere. Environmental Science & Technology 50 (3), 1280–1287. https://doi.org/10.1021/acs.est.5b05148.

King, A.C.F., Thomas, E.R., Pedro, J.B., Markle, B., Potocki, M., Jackson, S.L., Wolff, E., Kalberer, M., 2019. Organic Compounds in a sub-Antarctic ice core: a potential suite of sea ice markers. Geophys. Res. Lett. 46 (16), 9930–9939. https://doi.org/10.1029/2019GL084249.

Krnavek, L., Simpson, W.R., Carlson, D., Domine, F., Douglas, T.A., Sturm, M., 2012. The chemical composition of surface snow in the Arctic: examining marine, terrestrial, and atmospheric influences. Atmos. Environ. 50, 349–359. https://doi.org/10.1016/j.atmosenv.2011.11.033.

Li, Q., Tham, Y.J., Fernandez, R.P., He, X., Cuevas, C.A., Saiz-Lopez, A., 2022. Role of iodine recycling on sea-salt aerosols in the global marine boundary layer. Geophys. Res. Lett. 49 (6) https://doi.org/10.1029/2021GL097567.

Liu, S., Liu, C.-C., Froyd, K.D., Schill, G.P., Murphy, D.M., Bui, T.P., Dean-Day, J.M., Weinzierl, B., Dollner, M., Diskin, G.S., Chen, G., Gao, R.-S., 2021. Sea spray aerosol concentration modulated by sea surface temperature. Proc. Natl. Acad. Sci. 118 (9). https://doi.org/10.1073/pnas.2020583118.

Lovenduski, N.S., 2005. Impact of the southern Annular mode on Southern Ocean circulation and biology. Geophys. Res. Lett. 32 (11), L11603 https://doi.org/10.1029/2005GL022727.

Maffezzoli, N., Spolaor, A., Barbante, C., Bertò, M., Frezzotti, M., Vallelonga, P., 2017. Bromine, iodine and sodium in surface snow along the 2013 Talos Dome-GV7 traverse (northern Victoria Land, East Antarctica). Cryosphere 11 (2), 693–705. https://doi.org/10.5194/tc-11-693-2017.

Marelle, L., Thomas, J.L., Ahmed, S., Tuite, K., Stutz, J., Dommergue, A., Simpson, W.R., Frey, M.M., Baladima, F., 2021. Implementation and impacts of surface and blowing snow sources of arctic bromine activation within WRF-Chem 4.1.1. J. Adv. Model. Earth Syst. 13 (8) https://doi.org/10.1029/2020MS002391.

Markle, B.R., Steig, E.J., Roe, G.H., Winckler, G., McConnell, J.R., 2018. Concomitant variability in high-latitude aerosols, water isotopes and the hydrologic cycle. Nat. Geosci. 11 (11), 853–859. https://doi.org/10.1038/s41561-018-0210-9.

Mayewski, P.A., Lyons, W.B., Zielinski, G., Twickler, M., Whitlow, S., Dibb, J., Grootes, P., Taylor, K., Whung, P.-Y., Fosberry, L., Wake, C., Welch, K., 1995. An ice-core-based, late holocene history for the Transantarctic mountains, Antarctica. Antarct. Res. 67, 33–45. https://doi.org/10.1002/9781118668207.ch4.

Mayewski, P.A., Maasch, K.A., Dixon, D., Sneed, S.B., Oglesby, R., Korotkikh, E., Potocki, M., Grigholm, B., Kreutz, K., Kurbatov, A.v., Spaulding, N., Stager, J.C., Taylor, K.C., Steig, E.J., White, J., Bertler, N.A.N., Goodwin, I., Simões, J.C., Jaña, R., et al., 2013. West Antarctica's sensitivity to natural and human-forced climate change over the Holocene. J. Quat. Sci. 28 (1), 40–48. https://doi.org/10.1002/jqs.2593.

Mayewski, P.A., Twickler, M.S., Whitlow, S.I., Meeker, L.D., Yang, Q., Thomas, J., Kreutz, K., Grootes, P.M., Morse, D.L., Steig, E.J., Waddington, E.D., Saltzman, E.S., Whung, P.-Y., Taylor, K.C., 1996. Climate change during the last deglaciation in Antarctica. Science 272 (5268), 1636–1638. https://doi.org/10.1126/science.272.5268.1636.

McConnell, J.R., Maselli, O.J., Sigl, M., Vallelonga, P., Neumann, T., Anschütz, H., Bales, R.C., Curran, M.A.J., Das, S.B., Edwards, R., Kipfstuhl, S., Layman, L., Thomas, E.R., 2014. Antarctic-wide array of high-resolution ice core records reveals pervasive lead pollution began in 1889 and persists today. Scientific Reports 4 (1), 5848. https://doi.org/10.1038/srep05848.

Moore, J.C., Grinsted, A., Kekonen, T., Pohjola, V., 2005. Separation of melting and environmental signals in an ice core with seasonal melt. Geophys. Res. Lett. 32 (10), L10501 https://doi.org/10.1029/2005GL023039.

Moser, D.E., Jackson, S., Kjær, H.A., Markle, B., Ngoumtsa, E., Pedro, J.B., Segato, D., Spolaor, A., Tetzner, D., Vallelonga, P., Thomas, E.R., 2021. An age scale for the first shallow (Sub-)Antarctic ice core from Young island, Northwest Ross sea. Geosciences 11 (9), 368. https://doi.org/10.3390/geosciences11090368.

Osman, M., Das, S.B., Marchal, O., Evans, M.J., 2017. Methanesulfonic acid (MSA) migration in polar ice: data synthesis and theory. Cryosphere 11 (6), 2439–2462. https://doi.org/10.5194/tc-11-2439-2017.

Peterson, P.K., Hartwig, M., May, N.W., Schwartz, E., Rigor, I., Ermold, W., Steele, M., Morison, J.H., Nghiem, S.V., Pratt, K.A., 2019. Snowpack measurements suggest role for multi-year sea ice regions in Arctic atmospheric bromine and chlorine chemistry. Elementa: Science of the Anthropocene 7. https://doi.org/10.1525/elementa.352.

Potocki, M., Mayewski, P.A., Kurbatov, A.V., Simões, J.C., Dixon, D.A., Goodwin, I., Carleton, A.M., Handley, M.J., Jaña, R., Korotkikh, E.V., 2016. Recent increase in Antarctic Peninsula ice core uranium concentrations. Atmos. Environ. 140, 381–385. https://doi.org/10.1016/j.atmosenv.2016.06.010.

Prados-Roman, C., Cuevas, C.A., Hay, T., Fernandez, R.P., Mahajan, A.S., Royer, S.-J., Galí, M., Simó, R., Dachs, J., Großmann, K., Kinnison, D.E., Lamarque, J.-F., Saiz-Lopez, A., 2015. Iodine oxide in the global marine boundary layer. Atmos. Chem. Phys. 15 (2), 583–593. https://doi.org/10.5194/acp-15-583-2015.

Pratt, K.A., Custard, K.D., Shepson, P.B., Douglas, T.A., Pöhler, D., General, S., Zielcke, J., Simpson, W.R., Platt, U., Tanner, D.J., Huey, L.G., Carlsen, M., Stirm, B.H., 2013. Photochemical production of molecular bromine in Arctic surface snowpacks. Nat. Geosci. 6 (5), 351–356. https://doi.org/10.1038/ngeo1779.

Purich, A., Doddridge, E.W., 2023. Record low Antarctic sea ice coverage indicates a new sea ice state. Communications Earth & Environment 4 (1), 314. https://doi.org/10.1038/s43247-023-00961-9.

Saiz-Lopez, A., Blaszczak-Boxe, C.S., Carpenter, L.J., 2015. A mechanism for biologically induced iodine emissions from sea ice 15, 9731–9746. https://doi.org/10.5194/acp-15-9731-2015.

Saiz-Lopez, A., von Glasow, R., 2012. Reactive halogen chemistry in the troposphere. Chem. Soc. Rev. 41 (19), 6448–6472. https://doi.org/10.1039/c2cs35208g.

Schönhardt, A., Begoin, M., Richter, A., Wittrock, F., Kaleschke, L., Gómez Martín, J.C., Burrows, J.P., 2012. Simultaneous satellite observations of IO and BrO over Antarctica. Atmos. Chem. Phys. 12 (14), 6565–6580. https://doi.org/10.5194/acp-12-6565-2012.

Schüpbach, S., Fischer, H., Bigler, M., Erhardt, T., Gfeller, G., Leuenberger, D., Mini, O., Mulvaney, R., Abram, N.J., Fleet, L., Frey, M.M., Thomas, E., Svensson, A., Dahl-Jensen, D., Kettner, E., Kjaer, H., Seierstad, I., Steffensen, J.P., Rasmussen, S.O., et al., 2018. Greenland records of aerosol source and atmospheric lifetime changes from the Eemian to the Holocene. Nat. Commun. 9 (1) https://doi.org/10.1038/s41467-018-03924-3.

Sen Gupta, A., England, M.H., 2006. Coupled Ocean–Atmosphere–Ice response to variations in the southern Annular mode. J. Clim. 19 (18), 4457–4486. https://doi.org/10.1175/JCLI3843.1.

Severi, M., Becagli, S., Caiazzo, L., Ciardini, V., Colizza, E., Giardi, F., Mezgec, K., Scarchilli, C., Stenni, B., Thomas, E.R., Traversi, R., Udisti, R., 2017. Sea salt sodium record from Talos Dome (East Antarctica) as a potential proxy of the Antarctic past sea ice extent. Chemosphere 177, 266–274. https://doi.org/10.1016/j.chemosphere.2017.03.025.

Simpson, W.R., Alvarez-Aviles, L., Douglas, T.A., Sturm, M., Domine, F., 2005. Halogens in the coastal snow pack near Barrow, Alaska: evidence for active bromine air-snow chemistry during springtime. Geophys. Res. Lett. 32 (4) https://doi.org/10.1029/2004GL021748.

Simpson, W.R., Von Glasow, R., Riedel, K., Anderson, P., Ariya, P., Bottenheim, J., Burrows, J., Carpenter, L.J., Frieß, U., Goodsite, M.E., Heard, D., Hutterli, M., Jacobi, H.W., Kaleschke, L., Neff, B., Plane, J., Platt, U., Richter, A., Roscoe, H., et al., 2007. Halogens and their role in polar boundary-layer ozone depletion. Atmos. Chem. Phys. 7 (16), 4375–4418. https://doi.org/10.5194/acp-7-4375-2007.

Sneed, S.B., Mayewski, P.A., Dixon, D.A., 2011. An emerging technique: multi-ice-core multi-parameter correlations with Antarctic sea-ice extent. Ann. Glaciol. 52 (PART 2), 347–354. https://doi.org/10.3189/172756411795931822, 57.

Spolaor, A., Burgay, F., Fernandez, R.P., Turetta, C., Cuevas, C.A., Kim, K., Kinnison, D. E., Lamarque, J.F., de Blasi, F., Barbaro, E., Corella, J.P., Vallelonga, P., Frezzotti, M., Barbante, C., Saiz-Lopez, A., 2021. Antarctic ozone hole modifies iodine geochemistry on the Antarctic Plateau. Nat. Commun. 12 (1), 1–9. https://doi.org/10.1038/s41467-021-26109-x.

Spolaor, A., Vallelonga, P., Gabrieli, J., Kehrwald, N., Turetta, C., Cozzi, G., Poto, L., Plane, J.M.C., Boutron, C., Barbante, C., 2013. Speciation analysis of iodine and bromine at picogram-per-gram levels in polar ice. Anal. Bioanal. Chem. 405 (2–3), 647–654. https://doi.org/10.1007/s00216-012-5806-0.

Spolaor, A., Vallelonga, P., Turetta, C., Maffezzoli, N., Cozzi, G., Gabrieli, J., Barbante, C., Goto-Azuma, K., Saiz-Lopez, A., Cuevas, C.A., Dahl-Jensen, D., 2016. Canadian arctic sea ice reconstructed from bromine in the Greenland NEEM ice core. Sci. Rep. 6 (August), 1–8. https://doi.org/10.1038/srep33925.

Stammerjohn, S.E., Scambos, T.A., 2020. Warming reaches the south Pole. Nat. Clim. Change 10 (8), 710–711. https://doi.org/10.1038/s41558-020-0827-8.

Thomas, E.R., Tetzner, D., Markle, B., Pedro, J., Gacitúa, G., Moser, D.E., Jackson, S., 2023. The first firn core from Peter 1st Island – capturing climate variability across the Bellingshausen Sea. EGUsphere. https://doi.org/10.5194/egusphere-2023-1064.

Thomas, E.R., Allen, C.S., Etourneau, J., King, A.C.F., Severi, M., Winton, V.H.L., Mueller, J., Crosta, X., Peck, V.L., 2019. Antarctic sea ice proxies from marine and ice core archives suitable for reconstructing sea ice over the past 2000 years. Geosciences 9 (12). https://doi.org/10.3390/geosciences9120506.

Thomas, E.R., Gacitúa, G., Pedro, J.B., Constance Faith King, A., Markle, B., Potocki, M., Elisabeth Moser, D., 2021. Physical properties of shallow ice cores from Antarctic and sub-Antarctic islands. Cryosphere 15 (2), 1173–1186. https://doi.org/10.5194/tc-15-1173-2021.

Thomas, E.R., Vladimirova, D.O., Tetzner, D., Daniel Emanuelsson, B., Chellman, N., Dixon, D.A., Goosse, H., Grieman, M.M., Sigl, M., Udy, D.G., Vance, T.R., Winski, D. A., Holly, V.L., Bertler, N.A., Hori, A., Laluraj, C., Motizuki, Y., Takahashi, K., Motoyama, H., et al., 2022. Ice core chemistry database: an Antarctic compilation of 1 sodium and sulphate records spanning the past 2000 years. Earth Syst. Sci. Data Discuss. https://doi.org/10.5194/essd-2022-368.

Thomas, M.A., Devasthale, A., Kahnert, M., 2022. Marine aerosol properties over the Southern Ocean in relation to the wintertime meteorological conditions. Atmos. Chem. Phys. 22 (1), 119–137. https://doi.org/10.5194/acp-22-119-2022.

Thompson, D.W.J., Solomon, S., Kushner, P.J., England, M.H., Grise, K.M., Karoly, D.J., 2011. Signatures of the Antarctic ozone hole in Southern Hemisphere surface climate change. Nat. Geosci. 4 (11), 741–749. https://doi.org/10.1038/ngeo1296.

Toom-Sauntry, D., Barrie, L.A., 2002. Chemical composition of snowfall in the high Arctic: 1990–1994. Atmos. Environ. 36 (15–16), 2683–2693. https://doi.org/10.1016/S1352-2310(02)00115-2.

Turner, J., Phillips, T., Thamban, M., Rahaman, W., Marshall, G.J., Wille, J.D., Favier, V., Winton, V.H.L., Thomas, E., Wang, Z., Broeke, M., Hosking, J.S., Lachlan-Cope, T., 2019. The dominant role of extreme precipitation events in Antarctic snowfall variability. Geophys. Res. Lett. 46 (6), 3502–3511. https://doi.org/10.1029/2018GL081517.

Vallelonga, P., Maffezzoli, N., Saiz-Lopez, A., Scoto, F., Kjær, H.A., Spolaor, A., 2021. Sea-ice reconstructions from bromine and iodine in ice cores. Quat. Sci. Rev. 269, 107133 https://doi.org/10.1016/j.quascirev.2021.107133.

Walton, D.W.H., Thomas, J., 2018. Cruise report - Antarctic Circumnavigation expedition (ACE) 20th december 2016 - 19th march 2017. https://doi.org/10.5281/zenodo.1443511.

Welch, K.A., Mayewski, P.A., Whitlow, S.I., 1993. Methanesulfonic acid in coastal Antarctic snow related to sea-ice extent. Geophys. Res. Lett. 20 (6), 443–446. https://doi.org/10.1029/93GL00499.

Weller, R., Traufetter, F., Fischer, H., Oerter, H., Piel, C., Miller, H., 2004. Postdepositional losses of methane sulfonate, nitrate, and chloride at the European Project for Ice Coring in Antarctica deep-drilling site in Dronning Maud Land, Antarctica. J. Geophys. Res. Atmos. 109 (7), 1–9. https://doi.org/10.1029/2003jd004189.

Wolff, E.W., Fischer, H., Fundel, F., Ruth, U., Twarloh, B., Littot, G.C., Mulvaney, R., Röthlisberger, R., de Angelis, M., Boutron, C.F., Hansson, M., Jonsell, U., Hutterli, M. A., Lambert, F., Kaufmann, P., Stauffer, B., Stocker, T.F., Steffensen, J.P., Bigler, M., et al., 2006. Southern Ocean sea-ice extent, productivity and iron flux over the past eight glacial cycles. Nature 440 (7083), 491–496. https://doi.org/10.1038/nature04614.

Yadav, J., Kumar, A., Mohan, R., 2022. Atmospheric precursors to the Antarctic sea ice record low in February 2022. Environmental Research Communications 4 (12), 121005. https://doi.org/10.1088/2515-7620/aca5f2.